Journal of Industrial and Engineering Chemistry 120 (2023) 332–339

Contents lists available at ScienceDirect

Journal of Industrial and Engineering Chemistry

journal homepage: www.elsevier.com/locate/jiec

Sustainable mold biomachining for the manufacturing of microfluidic devices

Arrate Santaolalla [a], Yara Alvarez-Braña [b,c], Astrid Barona [d], Lourdes Basabe-Desmonts [c,e], Fernando Benito-Lopez [b,*], Naiara Rojo [a,*]

[a] Department of Chemical and Environmental Engineering, Faculty of Engineering Vitoria-Gasteiz, University of the Basque Country UPV/EHU, c. Nieves Cano s/n, Vitoria-Gasteiz 01006, Spain
[b] Microfluidics Cluster UPV/EHU, Analytical Microsystems & Materials for Lab-on-a-Chip Group, Analytical Chemistry Department, University of the Basque Country UPV/EHU, Barrio Sarriena s/n, Leioa 48940, Spain
[c] Microfluidics Cluster UPV/EHU, BIOMICs microfluidics Research Group, Lascaray Research Center, University of the Basque Country UPV/EHU, av. Miguel de Unamuno 3, Vitoria-Gasteiz 01006, Spain
[d] Department of Chemical and Environmental Engineering, Faculty of Engineering Bilbao, University of the Basque Country UPV/EHU, plza. Torres Quevedo 1, Bilbao 48013, Spain
[e] Basque Foundation of Science, IKERBASQUE, c. María Díaz de Haro 3, Bilbao 48013, Spain

ARTICLE INFO

Article history:
Received 29 September 2022
Revised 24 November 2022
Accepted 23 December 2022
Available online 28 December 2022

Keywords:
Biomachining
Microfluidic devices
Metallic molds
Acidithiobacillus ferrooxidans
Pattern etching
Biotechnological mold manufacturing

ABSTRACT

Biomachining has been investigated as a sustainable and effective alternative to conventional prototyping techniques for molding polymeric materials for their subsequent use as microfluidic devices. A novel and simple process based on the combination of a Pressure Sensitive Adhesive mask and a varnish has been proposed for preparing metal workpieces as an alternative to photolithography, with the latter being the most widely used technique for protecting workpieces. As far as the bioprocess is concerned, it has been applied in successive mold-etching and oxidant bio-regeneration stages. Metal solubilization has proven to be repeatable in several consecutive mold-etching stages when using the regenerated oxidant solution. As a result, the lifespan of the biomachining medium has been prolonged, contributing to process sustainability. An equation with two restrictions has been proposed to predict the time required to obtain a mold with a fixed height, as metal solubilization evolves differently between the first and subsequent hours. Finally, the bio-engraved copper pieces have acted as effective molds in the fabrication of self-powered polydimethylsiloxane microfluidic devices. This new biomachining application is therefore an effective and ecofriendly process for producing microfluidic devices.

Introduction

The demand for more sustainable manufacturing processes has focused attention on biotechnological techniques for etching micropatterns on metallic surfaces [1,2]. As opposed to mechanical methods, the use of readily available microorganisms is low energy-consuming, and no thermal damage or residual stress is caused as the process does not exert any cutting pressure [3,4]. In addition, the biomachining or microorganism-assisted process is considered cost effective and more ecofriendly than conventional mechanical and chemical micromachining alternatives [5,6].

This process was first described in 1996 [7], with the extremely acidophilic bacterium *Acidithiobacillus ferrooxidans (A. ferrooxidans)* being the most widely used microorganism. One of the most remarkable characteristics of the process is that it follows a theoretically endless cycle in which the selective solubilization of the metal workpiece and oxidant regeneration take place simultaneously, contributing to process sustainability [8,9]. Nevertheless, factors such as bacterial inhibition by the increasing concentration of the dissolved metal [10,11] and the loss of the oxidant by the precipitation of iron-hydroxy sulfates [12,13] have been reported to hinder the overall process, resulting in a progressive decrease in the specific metal removal rate (SMRR) over time [5,9,14,15]. In order to achieve a stable and controlled biomachining process, Diaz-Tena et al. [9] have proposed introducing a regeneration step for the complete biological recovery of the oxidant after a short biomachining period. In this study, the bioregenerated Fe^{3+} was able to biomachine a copper piece during 1 h while maintaining the initial SMRR, but the strategy's long-term performance has not been assessed in detail yet. Extending the lifespan of the

* Corresponding authors.
E-mail addresses: fernando.benito@ehu.eus (F. Benito-Lopez), naiara.rojo@ehu.eus (N. Rojo).

https://doi.org/10.1016/j.jiec.2022.12.040
1226-086X/

biomachining solution (BM solution) is an alternative that would reduce the consumption of chemical reagents and waste generation, having a positive impact on the sustainability of the biomachining and circular economy.

Photolithography is the conventional technique widely used for generating a patterned coating on a metallic surface [1,2,16]. This technique requires different kinds of equipment and reagents for the subsequent steps (surface polishing and cleaning, coating with a photoresist layer, soft bake, UV exposure, post-exposure bake and development), whereby biomachining would benefit from the development of a simpler procedure for workpiece preparation. As far as the machined geometries are concerned, the etching of circular and triangular dimples [2,3], circular micro pillars [2,3], lines [1,17], squares [1], and rectangles [1] has already been reported. Although more complex structures, such as a gear-shaped island [1] and a micro-mixing system [16] have also been achieved, it should be noted that, to the best of the authors' knowledge, only one study has used biomachined copper pieces to manufacture a functional device [18].

Regardless of its high potential, this biotechnique has hardly been explored in the Lab-on-a-Chip (LOC) field, which plays a crucial role in the development of innovative technological advances in chemical, biological, and engineering operations. In this area, polydimethylsiloxane (PDMS) molding by soft-lithography is still the most widespread method for creating features and microchannels with geometries defined by a mold's structure [19,20]. This technique, however, involves numerous steps for producing the mold and actually molding the PDMS device, and requires the use of cleanroom facilities for generating small features.

Despite the progress made at research level, the microfluidic industry still requires the use of highly resistant molds for manufacturing large batches of devices with the same mold, for instance for the hot embossing of polymers [21]. Other rapid prototyping techniques for molding polymeric materials are therefore being studied with a view to reducing production time and cost [22]. In particular, metallic molds are rendering promising results as they are very resistant and can be used repeatedly, although machining techniques need to be applied for their fabrication [23]. To the best of the authorś knowledge, the preparation of biomachined metal molds for the manufacturing of PDMS microfluidic devices with well controlled microchannel dimensions has not yet been reported, even though this bioprocess has advantages over conventional techniques. For instance, physical and chemical machining (micro-milling, micro-EDM, chemical-etching, etc.) may compromise the molds properties and prompt environmental issues due to the hazardous chemicals needed and wastes generated during the fabrication process. In addition, these treatments make the control of the thickness of the layer eroded from the surface more laborious, hindering the standardization of the process for microfluidic applications [24]. By contrast, and in addition to its environmental benefits, biomachining allows a better control of the metal removal rate during the process, whereby molds with multiple dimensional features can be repeatedly applied for the fabrication of PDMS microfluidic devices.

This study focuses on the development of a two-step biomachining process for engraving well-defined microfluidic structures on a copper piece. Concerning the workpiece, the preparation procedure combines a Pressure Sensitive Adhesive (PSA) and a protective varnish as an alternative to photolithography. The biomachining process is divided into a bio-regeneration step and the subsequent re-use of the solution for the piece biomachining, with the aim being to achieve a repetitive mold-etching procedure and extend the life-span of the oxidizing solution. Finally, as proof of concept, the engraved molds are used for the fabrication of functional PDMS microfluidic devices.

Materials and methods

Microorganisms and biomachining solution

The acidophilic bacterium *A. ferrooxidans* DSM 14882 selected for this study was acquired from the Leibniz Institute DSMZ-German Collection of Microorganisms and Cell Cultures.

The BM solution was prepared by culturing the bacteria in the nutrient medium developed by Lundgren-Silverman [25] until the complete oxidation of Fe^{2+} to Fe^{3+}. Thus, 5 % (v/v) of an *A. ferrooxidans* culture in an exponential growth phase was inoculated in 150 mL of the nutrient media containing 9 g/L of Fe^{2+}. Bacterial growth was carried out in an orbital incubator (Shaking Incubator 211B) at 130 rpm and 31 °C, and the pH of the solution was adjusted to 1.8 with sulfuric acid (25 % v/v).

The abiotic machining solution (M solution) used for comparison purposes in the control tests was obtained by filtering the BM solution with a 0.45 μm polyvinylidene fluoride filter for bacterial removal.

Workpiece preparation and masking

Flat copper (Cu^0) workpieces measuring 32 × 25 × 2 mm and 99.9 % purity were cut in the Department of Mechanical Engineering at the University of the Basque Country UPV/EHU (Spain), using a REMET TRE100 Evol metallographic saw.

The workpieces were prepared according to the novel coating process based on the combination of a PSA mask and a protective varnish to ensure that only the side with the geometry to be engraved was exposed to the BM solution.

Two geometries were designed to be engraved on the copper workpieces: a circle of 10 mm diameter and a microfluidic serpentine channel (72 mm total length × 2 mm width) that included an inlet circle and two outlet circles of 3 mm diameter. The masks were cut by Graphtec cutting Plotter CE6000-40 (CPS Cutter Printer Systems, Spain) on sheets of PSA (127 μm thick ARcare® 8939 white PSA, Adhesive Research, Ireland). Each copper workpiece was rinsed with deionized water and ethanol (96 %), and gently wiped to remove surface moisture. The PSA mask (circle or serpentine channel) was then stuck to the surface, so only the metal from the uncovered area was removed when immersing the piece in the BM solution.

Before further treatment, the back of each workpiece was covered with a protective varnish (MONGAY, S.A.) to ensure that only the side with the geometry to be engraved was exposed to the oxidizing solution. The efficiency of the varnish for preventing the etching of the material surface without inhibiting bacterial growth was tested prior to use. The inert material selected for these experiments was a rod glass, as any other metallic material could interfere with the process. A glass rod coated with the varnish was therefore immersed by suspension into 150 mL of nutrient medium inoculated with a 5 % (v/v) *A. ferrooxidans* culture in the exponential growth phase, and incubated at 130 rpm and 31 °C until all the Fe^{2+} was oxidized into Fe^{3+}. Once all the ferrous iron had been oxidized, the coated rod was maintained submerged in the BM solution for 24 h to ascertain whether the varnish reacted with the oxidizing agent (Fe^{3+}). The control sample was an Erlenmeyer containing solely an inoculated culture medium (with no rod immersed). The evolution of the iron species (total, Fe^{2+} and Fe^{3+}) and pH were measured throughout the experiment. In addition, the weight loss of the coated rod was measured after immersion in the BM solution for 24 h.

Influence of treatment time on mold-etching

The relationship between biomachining time and both the SMRR and the height of the engraved structure was studied in

two mold-etching experiments. First, two copper workpieces (Cu^0) masked with the circular geometry were immersed for 7 h in 150 mL of the BM (biotic) and M (abiotic) solution, respectively. After several time intervals (i.e., 0.25, 0.50, 0.75, 1.00, 2.00, 3.00, 4.00, 5.00, 6.00, and 7.00 h), each workpiece was removed from the treatment solution, rinsed with ethanol (96 %) and deionized water, dried, weighed (Denver instruments, SI-234), and immersed again in the same solution for the next biomachining period.

The second experiment involved the use of the mask with the microfluidic structure. Five different copper workpieces were partially covered with the PSA serpentine channel, and then each piece was subjected to one of following treatment times: 0.25, 0.50, 1.00, 2.00, and 6.00 h.

Both experiments were carried out in an orbital incubator (Shaking Incubator 211B) at 130 rpm and 31 °C. The pH was measured and, if necessary, adjusted to 1.8 during the process by adding sulfuric acid (25 % v/v). All the assays were carried out by duplicate and under non-sterile conditions to simulate a real-scale process.

Lifespan extension of the BM solution

Several consecutive mold-etching plus Fe^{2+} re-oxidation (oxidant regeneration) cycles were carried out to study the reliability of the process when re-using the BM solution (instead of using fresh solution), and to explore the microorganisms' ability to regenerate the medium at high copper concentrations. The study also assessed the influence of the regenerated BM solution on both the average SMRR and the engraved height after successive mold-etching plus regeneration cycles. For this purpose, copper workpieces masked with the microfluidic channel were selected. Fig. 1 shows the schematics of the two-stage process proposed in this experiment for mold fabrication. Stage 1, involving the mold-etching (biomachining) process, was carried out under the same experimental conditions described in the previous section. After each treatment time (0.25, 0.50, 2.00, and 6.00 h), Stage 2 involved the extraction of the workpiece (Cu^0) from the BM solution to let the microorganisms regenerate the oxidant. Once regeneration had been completed, that is, when all the Fe^{2+} was converted to Fe^{3+}, the same copper workpiece was immersed again in this regenerated solution for the next mold-etching step. The process was cyclically repeated until the time needed for Fe^{2+} re-oxidation doubled the time required in the first regeneration step.

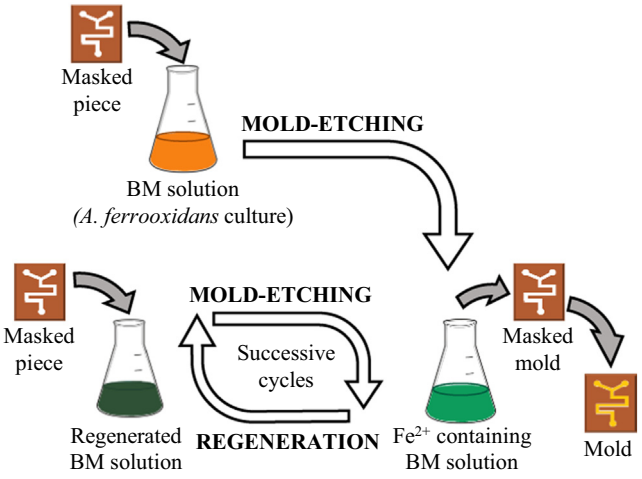

Fig. 1. Schematics of the mold-etching plus oxidant regeneration process for the generation of the molds required in the fabrication of PDMS microfluidic devices.

Fabrication of self-powered PDMS devices

Once the copper mold-etching had been completed, the PSA mask was removed from the surface and the metal piece was placed inside of a poly(methyl methacrylate) (PMMA) gasket. The gasket, consisting of two different PMMA substrates glued with a transparent PSA layer, was grafted by a CO_2 Laser System (VERSA Laser, VLS2.30 Desktop Universal Laser System equipped with a 10.6 μm CO_2 laser source ranging in power from 10 to 30 watts). A 1.1 mm thick PMMA substrate (ME303010, clear, Goodfellow) was cut (37 mm length × 30 mm width) and used as the base of the device. A 4 mm thick PMMA substrate (PLEXIGLAS®, Evonik Industries AG) was used for the gasket walls, delimiting an internal space of 32 mm length × 25 mm width for holding the metal mold. The transparent PSA layer (146 μm thick ARcare® 90880, Adhesive Research, Ireland) used for attaching the two pieces of PMMA was cut by the same Graphtec Cutting Plotter as described above for the PSA.

The PDMS devices were fabricated by casting, placing the copper mold inside of the PMMA gasket. The curing agent and the polymer-base (SYLGARD 184 silicone elastomer kit, Farnell, Spain) were mixed (1:10 proportion) and degassed in a vacuum desiccator (Poly-Lab, Spain) for 30 min to remove air bubbles. Once degassed, the PDMS mixture was poured onto the gasket and placed at 70 °C in a STZ 5.4 mini oven (FALC, Italy) for 2 h, in order to completely cross-link the PDMS. The resulting PDMS device was peeled off the mold, and three through-holes were punched in the inlet and outlets of the device, using a 3.0 mm diameter Harris Uni-Core Punch (Sigma Aldrich, Spain) for loading the sample. The microchannel was closed using a transparent PSA layer (50 μm thick ARcare® 92712, Adhesive Research, Ireland) as the base of the device. For its self-power capabilities, the resulting PDMS device was degassed in an RVR003H-01Vacuum Chamber (Dekker Vacuum Technologies, USA) for 1 h at 0.7 mbar to remove the air inside the material, and then vacuum-packed using an SV-204 vacuum seal (Samic, Spain) to store it in an airless environment. This vacuum-packing allows storage and transport of the device for long periods of time, ready to use. When needed, the PDMS device is restored to atmospheric pressure by simply opening the package, and a sample (water + red dye) is added to the inlet. The PDMS absorbs air from the closed serpentine structure, moving the liquid sample through the entire channel, without the need for any external power pump supply [26].

Analytical methods

The content of iron (Fe^{2+} and Fe^{3+}) was determined by using the 2,2′-dipyridyl molecular absorption spectrophotometry method (after Fe^{3+} reduction when necessary) [9]. A Perkin Elmer AAnalyst 100 AAS equipment was also used to quantify the total amount of iron. The pH was measured with a Crison Basic 20 pH-meter equipped with a SENSION + 5010 T pH electrode.

The efficiency of the mold-etching step was quantified by calculating the SMRR as follows

$$\text{SMRR (mg h}^{-1}\text{ cm}^{-2}) = \frac{\text{Amount of metal removed (mg)}}{\text{time (h) area (cm}^2)} \quad (1)$$

The height of the micro-etched structures was measured using a stylus profilometer (DektakXT, Germany). The video (Supplementary Information II) was recorded by using a smartphone One-Plus 6 T, 1080p at 30 fps.

Results and discussion

Workpiece preparation: an alternative to traditional techniques

The alternative process for workpiece preparation proposed here arises from the need to simplify, shorten and reduce the cost

of this preliminary stage, as photolithography (the most used technique for selectively covering the pieces to be biomachined) is tedious, it requires the use of expensive masks and custom-made optical components, and the photoresins require stringent post-processing conditions [27]. Two readily available and affordable materials (a common varnish and a PSA substrate) were selected here to cover the workpiece and generate the desired geometry. The protective varnish did not interfere with the process or halt bacterial activity, as the time required for the complete bio-oxidation of Fe^{2+} in the sample containing the coated glass rod and the blank was 58 h in both cases. Furthermore, after 24 h submerged in the BM solution, when all the iron was Fe^{3+}, the mass loss in the protected glass rod was negligible (0.06 %). Likewise, visual inspection revealed that the PSA layers were not detached from the workpiece after 30 h of treatment, and successfully covered the desired surface.

The circular PSA mask was used to monitor the original dimensions of the geometry throughout the treatment. The variation in the diameter of the circular structure engraved was measured after 7 h, and it was lower than 3 % compared to the original value (1 cm), both in the biotic (0.98 ± 0.01 cm) and abiotic (0.97 ± 0.0 1 cm) samples. Based on these results, the process was not considered to affect the original geometry. Therefore, the varnish and PSA layer combination was concluded to be a feasible, biocompatible and cost-effective method for surface protection in biomachining applications. It was a simpler and much less time-consuming process than photolithography (the total pretreatment time was estimated to be 20 min, of which approximately 15 min corresponded to varnish drying time). In addition, it would allow the generation of 3D geometries of different heights by overlapping PSA masks at different treatment times. This would be a more feasible procedure than a planar technique such as photolithography [27], which requires repeating the full process after careful alignment over the previously generated feature.

Specific metal removal rate and height of workpiece as a function of treatment time

The circle mask was first selected to ascertain the influence of biomachining time on both the SMRR and the height of the structure. As shown in Fig. 2, the SMMR peaked after 1 h treatment which is in agreement with other authors [9,15].

Interestingly, the SMRR here remained constant at 21 ± 1 mg h^{-1} cm^{-2}, both in the presence and in the absence of microorganisms, when the biomachining time was equal to or shorter than 1 h (15, 30, 45, and 60 min) (Fig. 2). Consequently, the height of the engraved surface increased linearly with treatment time during the first hour at a rate of 18.8 μm h^{-1} (R^2 = 0.9675) and 18.6 μm h^{-1} (R^2 = 0.9678) in the biotic and abiotic samples, respectively. Three possible reactions can contribute to the copper oxidation. As far as the reaction between the dissolved oxygen and copper is concerned, and, despite the major difference in the standard reduction potentials between oxygen and copper (O_2/H_2O = 1.23 V vs Cu^{2+}/Cu^0 = 0.34 V), copper oxidation by dissolved oxygen has been considered negligible on the basis of the low oxygen solubility in water and the gas–liquid mass transfer limitations [28]. The second reaction between copper and Fe^{3+} as oxidizing agent through the indirect mechanism is shown in Eq. (2). The third reaction requires the presence of *A. ferrooxidans* bacterium so that it can use the previously generated Fe^{2+} as energy source, with the oxidant Fe^{3+} being bio-recovered (Eq. (3)). According to the literature about Eq. (3), most of the electrons (95 %) enter the downhill electron pathway during the oxidation process, accessing the cytoplasm through the cell membrane, transporting oxygen, and reacting with protons to generate water.

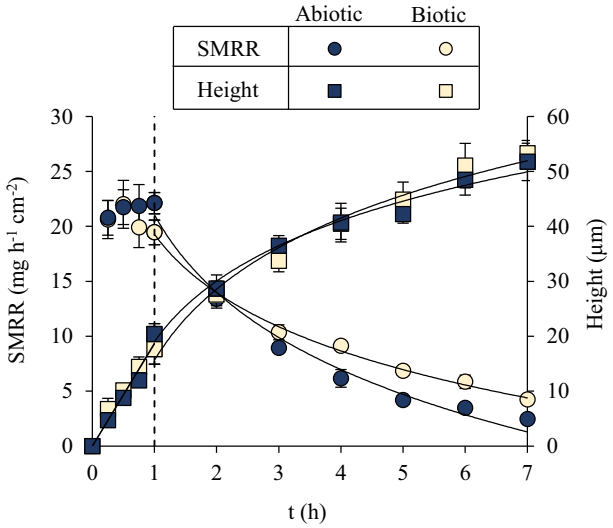

Fig. 2. Variation of the SMRR and height of the engraved structures throughout treatment time (0–7 h).

Simultaneously, a proton gradient is formed by pumping the protons out of the membrane [29,30].

$$2\ Fe^{3+} + Cu^0 \rightarrow 2\ Fe^{2+} + Cu^{2+} \quad (2)$$

$$4\ Fe^{2+} + 4H^+ + O_2 \rightarrow 4\ Fe^{3+} + 2\ H_2O \quad (3)$$

In the presence of bacteria, reactions in Eq. (2) and Eq. (3) can lead to a cyclic process in which copper is dissolved and Fe^{3+} bio-oxidized until the environmental conditions (e.g., pH and dissolved copper concentration) inhibit bacterial activity. Nevertheless, the biological Fe^{3+} regeneration (Eq. (3)) has been reported to be slower than its consumption (Eq. (2)) [28]. Thus, the results obtained during the shortest treatment times (when the SMRR resulted not to be affected by the presence of microorganisms) can be explained on the basis of the slow regeneration rate and the high amount of available oxidant.

After the first hour of treatment, the SMRR decreased following a logarithmic trend, and thus the height of the engraved circle increased accordingly. The regression equations correlating the SMRR, height, and removed copper according to the treatment time are listed in Supplementary Information I, see Table SI1. Similar results have been reported by Istiyanto et al. [14], who have found that the metal removal rate was inversely proportional to machining time, albeit not linear, when copper pieces are biomachined in the 9 K medium (35 °C, 120 rpm). The reduction in the SMRR can be mainly attributed to the gradual decrease in the oxidant concentration along time. In addition, other factors such as the increasing concentration of dissolved Cu^{2+} and the possible decrease in Fe^{3+} concentration due to the precipitation of iron-hydroxy sulfates can contribute to this behavior. Although copper is an essential element required by living organisms, when moderate concentrations (depending on the bacterial strain) are exceeded, this metal has been reported to severely inhibit bacterial activity by damaging cell membranes, altering enzyme specificity, disrupting cellular functions, and compromising the DNA structure [31,32]. Regarding oxidant loss, iron can be hydrolyzed and precipitated (when pH is higher than 2.0), reducing the available amount of dissolved Fe^{3+} for copper oxidation. The process can lead to the formation of hydroxy sulfates such as schwertmannite ($Fe_8O_8(OH)_6SO_4$) and jarosite ($MFe_3(SO_4)_2(OH)_6$; where M is usually Na^+, K^+, NH_4^+, or H_3O^+), and ferrihydrite, with the dominant phase being influenced by the pH and concentration of monovalent cations

[33,34]. Nevertheless, the total iron concentration here did not decay significantly throughout the experiment (0.5 g L^{-1} after 7 h of biomachining), whereby iron loss was not considered a critical factor.

Regarding the difference in the SMRR between the biotic and abiotic samples, after 3 h of biomachining, the SMRR was higher in the biotic samples than in the abiotic ones, which was attributed to the higher availability of Fe^{3+} regenerated by the bacteria (Eq. (3)). This difference remained 1.7 times higher in the biotic process from hour 5 onwards.

As far as mold height is concerned, values of 53 ± 2 and 52 ± 3 μm were recorded after 7 h in the biotic and abiotic experiments, respectively. These values cannot be accurately compared with the results reported by other authors, as most biomachining studies describe the generation of cavities with different shapes (circles, lines, etc.), whereby depth values are reported (instead of height). In addition, the results vary with operating parameters, such as the initial iron concentration or shaking speed. Nevertheless, for comparison purposes, Table 1 shows the height and depths reported by other authors when using *A. ferrooxidans* for biomachining several geometries on copper pieces.

Five treatment times (0.25, 0.50, 1.00, 2.00, and 6.00 h) were selected to verify that the two-trend behavior observed with the circular geometry remained constant when engraving a complex microfluidic structure. Moreover, this experiment informed the equations for calculating the treatment time required to achieve a desired height on the structure. In this case, each copper piece was continuously immersed in the BM solution for the selected time, without intermediate extractions. Thus, for comparison purposes, the data plotted in Fig. 2 were used to calculate the average SMRR for the same time intervals (0.25, 0.50, 1.00, 2.00, and 6.00 h) in the experiment carried out with the circular geometry.

Fig. 3 shows that the average SMRR was slightly higher for the microfluidic pattern than for the circular one during the first hour. Nevertheless, no significant differences were observed regarding the geometry of the engraved structure for longer treatments. In accordance with the results obtained with the circular geometry, a maximum average SMRR was recorded and maintained constant during the first hour (21 ± 1 and 23 ± 1 mg h^{-1} cm^{-2} for the circle and microfluidic channel, respectively). It then decreased in a logarithmic trend with treatment time, regardless of the shape of the structure (SMRR = -5.2·ln(t) + 20.6, R^2 = 0.9979, and SMRR = -6.4·ln (t) + 23.1, R^2 = 0.9993; for the circle and microfluidic channel, respectively).

Table 1
Heights and depths reported in the literature and in this study, when using *A. ferrooxidans* in copper biomachining experiments (T = 30–35 °C).

Geometry	Height/depth[a]	Shaking speed	Author
Lines	80 μm (48 h)	Static conditions	[17]
Circular gear	48 μm (24 h)	Static conditions	[1]
Line[b]	74.75 μm (4 h)	150 rpm	[35]
Circle[b]	61.75 μm (4 h)		
Square[b]	60.45 μm (4 h)		
Crescent dimples	14.65 μm (20 min)	170 rpm	[2]
Circular dimples	13.98 μm (20 min)		
Circular micro pillars	9.56 μm (100 min)		
Circle	51.1 μm (7 h)	130 rpm	This study
Microfluidic geometry	65.3 μm (6 h)		

[a] The value in parenthesis refers to biomachining time.
[b] the authors used the supernatant obtained after filtering the *A. ferrooxidans* culture (test without microorganisms).

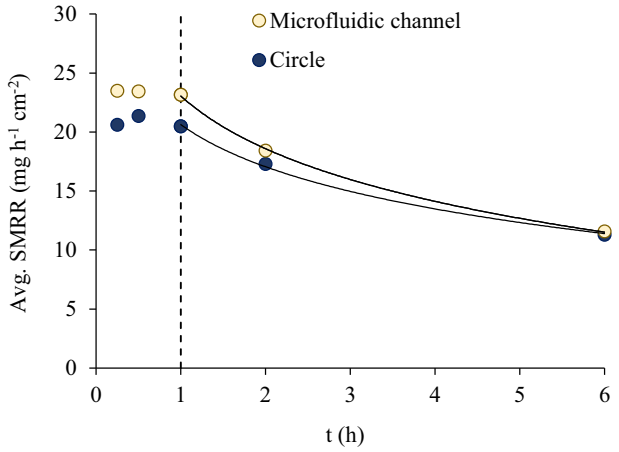

Fig. 3. Average SMRR values obtained after the selected treatment time in the samples with the circular geometry and microfluidic channels.

As far as the height of the mold is concerned, greater values were recorded in the experiments using the microfluidic structure than the circular geometry, which was attributed to the slightly higher average SMRR and the smaller surface area exposed to the solution. As an example, after a 6 h biomachining treatment, the height of the microchannel (64 ± 5 μm) was 28 % greater than that of the circle (51 ± 4 μm).

Based on these results achieved with the microfluidic structure, the equation for predicting the treatment time (h) needed to produce a serpentine channel mold of a certain height (H, μm) was calculated as follows (Eq. (4)):

$$t\begin{cases} 0.045 \cdot H;\ 0 \le t < 1\ h\ (R^2 = 0.9912) \\ 0.564 \cdot exp(0.036 \cdot H);\ 1 \le t \le 7\ h\ (R^2 = 0.9994) \end{cases} \quad (4)$$

This equation is a simple tool for readily calculating the biomachining time required for obtaining a specific engravement height in a microfluidic structure. Despite this practical calculation, the proposed equation revealed that mold fabrication by biomachining can be more time-consuming than other techniques. Nevertheless, many conventional techniques require exhaustive monitoring by qualified personnel during the entire process and/or the use of a cleanroom facility, considerably increasing the total cost of the process. Hence, the biologically assisted etching method was found to be low time-consuming for laboratory personnel, avoiding the need for pre-treatment. In addition, the biomachining alternative provides an accurate control of the resulting structure, allowing the height to be measured continuously during the mold-etching step. By contrast, taking photolithography as a reference model, the structural shape can be measured only when the full process has finished, ruling out any possible adjustments.

Lifespan extention of the BM solution for a more sustainable process

The regeneration step carried out after each mold-etching stage resulted in the complete microbial re-oxidation of the Fe^{2+} generated during the biomachining process. Fig. 4a shows the variation of Fe^{3+} in the sample treated for 0.5 h in seven mold-etching plus regeneration stages, as a representative example of the process. Following each regeneration stage, all the dissolved iron was in Fe^{3+} form, and the system was therefore ready to perform the next biomachining stage. The regenerated BM solution rendered similar results to those obtained in the single stage assay with a fresh solution. In addition, it is particularly remarkable for this application

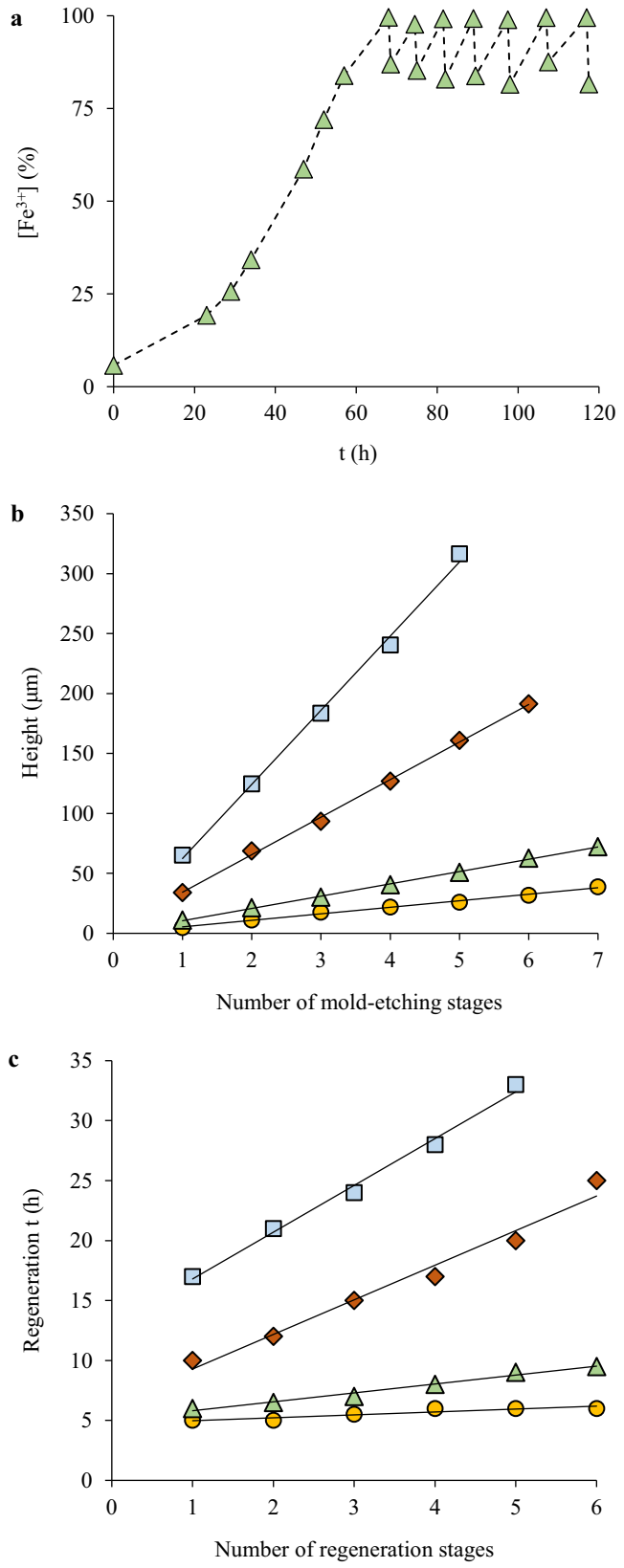

Fig. 4. Variation of Fe^{3+} (%) during several biomachining (0.5 h) and regeneration stages (a), evolution of the height of the mold with the number of mold-etching stages (b), and time needed for Fe^{2+} re-oxidation in each regeneration stage (c).

that the average SMRR remained constant for each treatment time in at least five to seven consecutive mold-etching stages. This interesting result ensured that the same amount of copper would be dissolved when a piece was exposed to the BM solution for a certain treatment time. In this study, the average SMRR peaked and remained constant at 24 ± 1 mg h^{-1} cm^{-2} in seven consecutive mold-etching steps when the treatment was shorter than 1 h. In longer treatments, 18 ± 1 and 10.9 ± 0.4 mg h^{-1} cm^{-2} were removed in the 2 h biomachining process (average of six consecutive stages) and the 6 h one (average of five consecutive stages), respectively. This outcome confirmed the accuracy of the equation proposed for predicting the time needed to obtain a mold with a defined height for the fabrication of PDMS devices (Eq. (4)), using both fresh and regenerated BM solutions. Consistent with these results (*i.e.* constant average SMRR for each treatment time), the increase in the height of the structure measured after each mold-etching time remained practically constant, being this increment of 5 ± 1, 10 ± 1, 32 ± 4 and 63 ± 8 µm for 0.25, 0.50, 2.00, and 6.00 h treatments, respectively. Consequently, as the successive etching stages progressed, the total height of the structure increased linearly (Fig. 4b, regression equations correlating height to the number of etching-stages are listed in Supplementary Information I, Table SI2). Copper solubilization during the process rendered an average metal mass dissolved in each mold-etching stage of 53 ± 3, 107 ± 10, 313 ± 23 and 571 ± 35 mg, recording 2.8, 5.8, 13.5 and 20.6 g Cu^{2+} L^{-1} at the end of the 0.25, 0.50, 2.00, and 6.00 h experiments, respectively (assuming that all the copper removed remained dissolved).

The reuse of the BM solution in several consecutive etching stages led to the successful fabrication of metallic molds, increasing the sustainability of the process from both an environmental and an economic perspective. The regeneration time was affected by both the duration of the mold-etching process (0.25, 0.50, 2.00 and 6.00 h), and the number of mold-etching plus regeneration cycles to which the microorganisms were subjected. The relationship between the regeneration time and the number of regeneration stage was found to be linear for each selected treatment time, as shown in Fig. 4c. Thus, the equations summarized in Table 2 would allow estimating the time required for a certain regeneration stage.

Regarding the influence of the duration of the etching stage, longer regeneration times were required for the longest biomachining processes (2.00 and 6.00 h) because of the higher amount of Fe^{2+} to be re-oxidized (Fig. 4c). For example, after the first mold-etching stage, the regeneration time was 3.4 times higher for the 6 h than for the 0.25 h treatment. Likewise, this parameter also increased with the number of treatment stages in all the samples, as higher amounts of dissolved copper in the medium affected the process.

Nevertheless, according to literature [36,37], the exposure of microorganisms to increasing copper concentrations may favor their acclimation to the metal. As an example, the regeneration time for 0.25 h and 0.5 h treatment increased about 17–20 % (in comparison to the first regeneration time), when the Cu^{2+} concentration in the medium was 2.4 g Cu^{2+}/L (it happened after the sixth and third etching stages, respectively). Conversely, as far as longer etching times are concerned, a similar increase in the regeneration time was recorded at higher copper concentrations (20 % increase at 4.2 g Cu^{2+}/L in the medium for the 2 h treatment and 24 %

Table 2
Linear equations correlating the regeneration time (t_{regen}, h) and the number of regeneration stage (R) for each treatment time.

Treatment time (h)	Fitting equation	R^2
0.25	t_{regen} = 4.7 + 0.3·R	0.9074
0.50	t_{regen} = 5.0 + 0.8·R	0.9877
2.00	t_{regen} = 6.4 + 6.4·R	0.9748
6.00	t_{regen} = 12.9 + 3.9·R	0.9928

increase at 7.9 g Cu^{2+}/L for the 6 h treatment). Along those two experiments (2.00 h and 6.00 h experiments), the biomass had to withstand higher copper concentrations since the first stage, which contributed to microbial acclimation.

In this study, the microorganisms continued regenerating the oxidant even when copper concentration was as high as 20.6 g Cu^{2+}/L. Our previous studies revealed that *A. ferrooxidans* strain DSM 14882 was able to successfully oxidize all the Fe^{2+} in the presence of up to 30 g Cu^{2+} L^{-1} in a significantly lower time than using unadapted bacteria [37]. Nevertheless, in this study, the experimentation was not prolonged because too long regeneration time could be to the detriment for the process feasibility.

In sum, the two-stage procedure proposed in this study had very positive implications for the sustainable fabrication of molds for PDMS microfluidic devices. The regeneration and reuse of the BM solution meant a reduction in both chemical reactant consumption and waste generation, with the consequent savings in process cost. In addition, the spent BM solution is a source of recoverable copper, which could finally be sold on the metal market [38–40].

Fabrication of self-powered PDMS devices

Self-powered devices provide the means to control liquids in the fluidic network without using any external pumping mechanisms, whereby the devices can be transported to the point of need and perform in situ analyses [26,41]. The use of a degassed gas-permeable silicone (such as PDMS) as the base material for the cartridge generates a negative pressure inside the microfluidic structure that permits the autonomous movement of the sample through the channel. Despite being the most commonly used self-powered devices [42], their manufacture by casting and molding is still complex and laborious. The molds produced with the biomachining process were therefore used for the manufacture of hybrid PDMS/PSA self-powered microfluidic devices. Fig. 5 describes the fabrication and performance of a microfluidic device made from a mold obtained after five cycles of 6 h biomachining plus solution regeneration (channel height 317 ± 5 µm). Other similar devices were also obtained with the molds biomachined in shorter times.

Surface roughness is a relevant parameter in biomachined molds [2,14,43,44], as it has an impact on the roughness of the final PDMS piece. The arithmetic average roughness (Ra) of copper molds with a simple geometry (circle) was found to be in the 1.9–2.5 µm range for a 30 h biomachining treatment, which was similar to the range reported by Johnson et al. [43] (1.8–2.6 µm for a 24 h treatment) and Istiyanto et al. [14] (1.5–1.8 µm for a 18 h treatment). This parameter has been reported not to vary linearly with treatment duration [14], which let us conclude that Ra values of the molds used for the fabrication of the microfluidic devices could be lower than those preliminarily obtained for 30 h. However, the surface roughness of the manufactured PDMS piece hindered the bonding of this replica to other PDMS or glass surfaces, even after plasma treatment of both surfaces. The PDMS replica was therefore closed using a PSA layer as a base for the device. The use of a PSA as the top layer of the device allowed closing the channel easily without the use of thermal or chemical bonds or surface treatments. As previously reported by our group, multi-laminated microfluidic devices adhered by PSA layers can withstand pressures up to 1000 mbar without suffering any damage [45]. This type of PDMS/PSA configuration should therefore be suitable for many microfluidic applications that do not require high pressures. In addition, the normal pressures generated by self-powered devices are much lower (e.g., 0.05–0.35 mbar) [26]. No leaching was observed for any of the devices investigated using this protocol.

Finally, the microfluidic piece was degasified to enable the self-powered device to circulate the liquid through the microchannel by degas-driven flow [46]. Accordingly, once the degasification was complete, the device was placed at atmospheric pressure, and one drop of a colored solution was added into the device. Fig. 5b1-3 and the video (Supplementary Information II) show how the liquid subsequently advanced through the entire serpentine in less than 3 min. This result confirms that the device's fluidic properties were not affected, despite the use of a hydrophobic substrate for the base (the PSA layer) for increasing flow resistance. Fig. 5b provides three snapshots of the movement of the red solution over time, though a 317 ± 5 µm high micro-channel obtained with a copper mold after a 6 h machining process.

The biomachined molding technique is a promising alternative for the manufacture of a variety of microfluidic devices with precise microchannel dimensions and a high performance. Nevertheless, further research is needed for stablishing the minimum dimensions that can be reached using this method. In this particular study, the minimum width of the microfluidic serpentine channel (100 µm) was limited by the plotter resolution, although smaller features could be obtained with other specific plotters. On-going research will let us deepen into the relevant parameters for commercial applications, such as: surface roughness, geometry scale limits, etc.

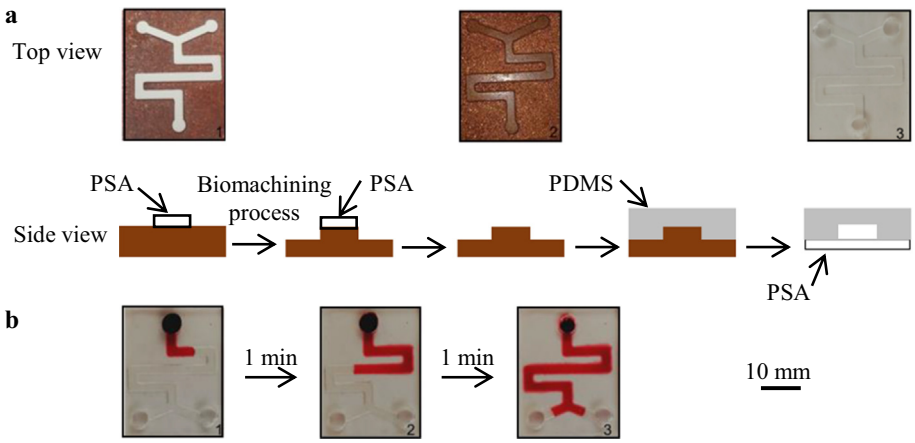

Fig. 5. Manufacture (a) and performance (b) of a hybrid PDMS/PSA microfluidic device (317 ± 5 µm height) after five cycles of 6 h biomachining plus solution regeneration.

Conclusions

The constant search for technologies that reduce the economic cost and environmental impact of conventional processes has led to the use of biomachining as an alternative for generating the molds required in the fabrication of microfluidic devices. The combination of a novel workpiece preparation procedure and the two-step biomachining process successfully rendered the engraving of durable and robust metallic molds, which were subsequently used for producing operative self-powered PDMS microfluidic devices. The biomachining technique did not require the use of a cleanroom facility, which is a clear advantage over conventional lithography methods.

Additionally, the replacement of the mask at different steps of the process could lead to the etching of more complex structures than the one presented here, which means catering for a variety of microstructures with different heights in the same mold. The particularity of the biomachining for controlling a high-precision metal removal rate at micrometer level in a short period of time was decisive for the successful manufacturing of microfluidic devices.

Declaration of Competing Interest

The authors declare that they have no known competing financial interests or personal relationships that could have appeared to influence the work reported in this paper.

Acknowledgements

This work was supported by the State Agency for Research (AEI) of the Spanish Government-European Regional Development Fund (FEDER-ERDF, EU) [grant number: CTM2016-77212-P], Spain's Ministry of Science and Education [grant number: PID2020-1203 13 GB-I00/AIE/10.13039/501100011033], and the Basque Government's Department of Education for the consolidation of research groups [grant number: IT1633-22]. Professor L. N. López de la Calle is acknowledged for his assistance with the copper samples.

Appendix A. Supplementary material

Supplementary data to this article can be found online at https://doi.org/10.1016/j.jiec.2022.12.040.

References

[1] J. Istiyanto, A.S. Saragih, T.J. Ko, Microelectron. Eng. 98 (2012) 561–565, https://doi.org/10.1016/j.mee.2012.07.002.
[2] I. Muhammad, T. Khatoon, S.M. Sana Ullah, T.J Ko. IJPEM-GT. 5 (2018) 201-209. https://doi.org/10.1007/s40684-018-0020-y.
[3] I. Muhammad, S.M. Sana Ullah, D.S. Han, T.J Ko. IJPEM-GT. 2 (2015) 307–313. https://doi.org/10.1007/s40684-015-0037-4.
[4] E. Diaz-Tena, G. Gallastegui, A. Barona, A. Rodríguez, L.N. López de Lacalle, A. Elías. Crit. Rev. Biotechnol. 37 (2017) 323-332. https://doi.org/10.3109/07388551.2016.1144046.
[5] E. Xenofontos, A. Feidiou, M. Constantinou, G. Constantinides, I. Vyrides, Corros. Sci. 100 (2015) 642–650, https://doi.org/10.1016/j.corsci.2015.08.041.
[6] T.S. Jhajj, A.K. Sodhi, N. Bhanot in: H. Singh, P. Garg, I. Kaur (Eds), Proceedings of the 1st International Conference on Sustainable Waste Management through Design. ICSWMD 2018. Lecture Notes in Civil Engineering, vol 21, Springer. 2019, pp. 323-335. https://doi.org/10.1007/978-3-030-02707-0_38.
[7] Y. Uno, T. Kaneeda, S. Yokomizo, JSME Int. J. 39 (1996) 837–842, https://doi.org/10.1299/jsmec1993.39.837.
[8] D. Zhang, Y. Li, Sci. China Ser. C 41 (1998) 151–156, https://doi.org/10.1007/BF02882720.
[9] E. Diaz-Tena, G. Gallastegui, M. Hipperdinger, E.R. Donati, M. Ramírez, A. Rodríguez, L.N. López de Lacalle, A. Elías. Corros. Sci. 112 (2016) 385-392. https://doi.org/10.1016/j.corsci.2016.08.001.
[10] N.C.S. Mykytczuk, J.T. Trevors, G.D. Ferroni, L.G. Leduc, Microbiol. Res. 166 (2011) 186–206, https://doi.org/10.1016/j.micres.2010.03.004.
[11] A. Mazuelos, C.J. García-Tinajero, R. Romero, N. Iglesias-González, F.J. Carranza. J. Chem. Technol. Biotechnol. 94 (2019) 185-194. https://doi.org/10.1002/jctb.5761.
[12] H. Wang, J.M. Bigham, O.H. Tuovinen. Mat. Sci. Eng. 26 (2006) 588-592. https://doi.org/10.1016/j.msec.2005.04.009.
[13] M. Yang, Y. Zhan, S. Zhang, W. Wang, L. Yan. 3 Biotech (2020), 10, 475. https://doi.org/10.1007/s13205-020-02463-3.
[14] J. Istiyanto, T.J. Ko, I.C. Yoon, IJPEM 11 (2010) 659–664, https://doi.org/10.1007/s12541-010-0077-1.
[15] U.U. Jadhav, H. Hocheng, W.H. Weng. J. Mater. Process. Technol. 213 (2013) 1509-1515. https://doi.org/10.1016/j.jmatprotec.2013.03.015.
[16] A. Singh, A. Manikandan, M.R. Sankar, K. Pakshirajan, L. Roy, in M. Shunmugam M. Kanthababu (Eds). Advances in Unconventional Machining and Composites. Lecture Notes on Multidisciplinary Industrial Engineering, Springer. Singapore, 2020, pp. 661-670.https://doi.org/10.1007/978-981-32-9471-4_55.
[17] J. Istiyanto, M.Y. Kim, T.J. Ko, Microelectron. Eng. 88 (2011) 2614–2617, https://doi.org/10.1016/j.mee.2011.02.004.
[18] M. Taufiqurrakhman, J. Istiyanto, N. Putra, TSEP 26 (2021), https://doi.org/10.1016/j.tsep.2021.101128.
[19] S. Torino, B. Corrado, M. Iodice, G. Coppola, Inventions 3 (2018) 65, https://doi.org/10.3390/inventions3030065.
[20] Y. Gao, G. Stybayeva, A. Revzin, Lab Chip 19 (2019) 306–315, https://doi.org/10.1039/C8LC00825F.
[21] S.S. Deshmukh, A. Goswami, Mater. Today-Proc. 26 (2020) 405–414, https://doi.org/10.1016/j.matpr.2019.12.067.
[22] M.A.M.M. Ferraz, J.B. Nagashima, B. Venzac, S. Le Gac, N. Songsasen. Sci. Rep. 10 (2020) 994, https://doi.org/10.1038/s41598-020-57816-y.
[23] E. Azarsa, M. Jeyhani, A. Ibrahim, S.S.H. Tsai, M. Papini, Biomicrofluidics 14 (2020), https://doi.org/10.1063/5.0009443.
[24] P.C. Pandey, H.S. Shan, Modern Machining Processes, Tata McGraw-Hill Publishers, India, 2012.
[25] M.P. Silverman, D.G. Lundgren. J. Bacteriol. 77 (1959) 642-647. https://doi.org/10.1128/jb.77.5.642-647.1959.
[26] J. Etxeberria-Elezgarai, Y. Alvarez-Braña, R. Garoz-Sanchez, F. Benito-Lopez, L. Basabe-Desmonts. Ind. Eng. Chem. Res. 59 (2020) 22485-22491. https://doi.org/10.1021/acs.iecr.0c03398.
[27] N. Liaros, J.T. Fourkas, Opt. Mater. Express 9 (2019) 3006–3020, https://doi.org/10.1364/OME.9.003006.
[28] F. Lambert, S. Gaydardzhiev, G. Léonard, G. Lewis, P.F. Bareel, D. Bastin. Miner. Eng. 76 (2015) 38-46. https://doi.org/10.1016/j.mineng.2014.12.029.
[29] S. Zhang, L. Yan, W. Xing, P. Chen, Y. Zhang, W. Wang, Extremophiles 22 (2018) 563–579, https://doi.org/10.1007/s00792-018-1024-9.
[30] J. Valdés, I. Pedroso, R. Quatrini, R.J. Dodson, H. Tettelin, R. Blake, J.A. Eisen, D.S. Holmes. BMC Genomics, 9 (2008) 597, https://doi.org/10.1186/1471-2164-9-597.
[31] M.R. Bruins, S. Kapil, F.W. Oehme. Ecotox. Environ. Safe. 45 (2000) 198-207. https://doi.org/10.1006/eesa.1999.1860.
[32] M. Valix., in: J.W.C. Wong, R.D. Tyagi, A. Pandey (Eds.), Current Developments in Biotechnology and Bioengineering, Elsevier, 2017, pp. 407-442. https://doi.org/10.1016/B978-0-444-63664-5.00018-6.
[33] J. Sanchez-España, in: Letcher, T.M. (Ed), Thermodynamics, Solubility and Environmental Issues, Elsevier Science. The Netherlands, 2007, pp. 137-150.
[34] Y. Song, L. Yang, H. Wang, X. Sun, S. Bai, N. Wang, J. Liang, L. Zhou, Environ. Technol. 42 (2021) 2325–2334, https://doi.org/10.1080/09593330.2019.1701564.
[35] H. Hocheng, J.H. Chang, U.U. Jadhav, J. Clean. Prod. 20 (2012) 180–185, https://doi.org/10.1016/j.jclepro.2011.07.019.
[36] G. Liang, W. Lin, Q. He, W. Liu, Q. Zhou. Environ. Prog. Sustain. Energy. 38 (2018) e13054, https://doi.org/10.1002/ep.13054.
[37] A. Santaolalla, J. Gutierrez, G. Gallastegui, A. Barona, N. Rojo. J. Environ. Chem. Eng. 9 (2021) 105283, https://doi.org/10.1016/j.jece.2021.105283.
[38] A.H. Kaksonen, L. Lavonen, M. Kuusenaho, A. Kolli, H. Närhi, E. Vestola, J.A. Puhakka, O.H. Tuovinen. Miner. Eng. 24 (2011) 1113-1121. https://doi.org/10.1016/j.mineng.2011.02.011.
[39] M. Ye, G. Li, P. Yan, J. Ren, L. Zheng, D. Han, S. Sun, S. Huang, Y. Zhong. Chemosphere. 185 (2017) 1189-1196. https://doi.org/10.1016/j.chemosphere.2017.07.124.
[40] A. Santaolalla, J. García, N. Rojo, A. Barona, G. Gallastegui, J. Clean. Prod. 270 (2020), https://doi.org/10.1016/j.jclepro.2020.122549.
[41] E.C. Yeh, C.C. Fu, L. Hu, R. Thakur, J. Feng, L.P. Lee. Sci. Adv. 3 (2017) e1501645, https://doi.org/10.1126/sciadv.1501645.
[42] I.K. Dimov, L. Basabe-Desmonts, J.L. Garcia-Cordero, B.M. Ross, A.J. Ricco, L.P. Lee. Lab Chip. 11 (2011) 845−850. https://doi.org/10.1039/C0LC00403K.
[43] D. Johnson, R. Warnes, A.J. Shih. J. Manuf. Sci. Eng. 129 (2007) 223-227. https://doi.org/10.1115/1.2401629.
[44] F. Ma, H. Huang, C. Cui. J. Mat. Process. Technol. 278 (2020) 116512, https://doi.org/10.1016/j.jmatprotec.2019.116512.
[45] J. Saez, L. Basabe-Desmonts, F. Benito-Lopez. Microfluid. Nanofluid. 20 (2016) 116, https://doi.org/10.1007/s10404-016-1781-7.
[46] D.Y. Liang, A.M. Tentori, I.K. Dimov, L.P. Lee. Biomicrofluidics. 5 (2011) 24108, https://doi.org/10.1063/1.3584003.